Rock Mech. Rock Engng. (2006) 39 (5), 421–444
DOI 10.1007/s00603-005-0078-z

Rock Mechanics and Rock Engineering
Printed in Austria

A Comparative Analysis of Pillar Design Methods and its Application to Marble Mines

By

C. González-Nicieza[1], **M. I. Álvarez-Fernández**[1], **A. Menéndez-Díaz**[2], and **A. E. Álvarez-Vigil**[3]

[1] Department of Mining Engineering, Mining Engineering School, University of Oviedo, Oviedo, Spain
[2] Department of Construction Engineering and Manufacturing, Mining Engineering School, University of Oviedo, Oviedo, Spain
[3] Department of Mathematics, Mining Engineering School, University of Oviedo, Oviedo, Spain

Received December 2, 2004; accepted November 30, 2005
Published online March 27, 2006

Summary

The methods for designing pillars in underground mines are fundamentally based on empirical formulae that do not take into account the quality of the rock mass as an input parameter. This makes them difficult to apply in other types of ground that are different to those used to establish each empirical formula.

To avoid this inconvenience, the present paper examines existing empirical formulae to then propose a modification of these formulae adjusting the resistance of the pillars on the basis of the RMR (Bieniawski's Rock Mass Rating). The compression safety factor of the pillars is analyzed for each modified formula and a study is carried out of shear failure if planes of weakness exist in the pillars. Finally, the safety factors of the pillars in a marble mine situated in Alicante (Southern Spain) were calculated in order to validate the new formulae.

From the results obtained, it is concluded that this new formulation determines the safety factor of pillars of the mine with greater reliability, provided that the pillars are isolated. At the same time, the introduction of the RMR in the formulae results in a better fit of the strength of each pillar to the characteristics of the rock mass.

Keywords: Pillar strength, failure criteria, intact rock, rock mass, RMR.

1. Introduction

Underground stone mining is an emerging sector of the mining industry. As this expansion takes mines under deeper cover, and as more efficient mining methods are employed, stone room-and-pillar design methods will become even more important.

Pillars can be defined as the in-situ rock mass between two or more underground openings. Hence, the construction of an underground mine will create pillars and rooms of variable geometries.

Stability issues associated with this kind of underground excavation in hard rock can be grouped into two general classes:

- Structurally controlled gravity-driven processes leading to wedge type failures.
- Stress-induced failure causing slabbing and spalling.

Structurally controlled gravity-driven failure usually involves wedge-type failures from the roof and sidewalls of the excavations. Such failures are generally found in areas of low confinement such as rooms, tunnel intersections or tunnels with straight walls or roofs.

As in-situ stress magnitudes increase, i.e. as the depth increases, natural fractures become clamped and the failure process becomes brittle and is dominated by new stress-induced fractures growing parallel to the excavation boundary. One of the key parameters characterizing brittle failure in hard rocks is the stress magnitude required to initiate and propagate these stress-induced fractures through intact or tightly clamped fractured rock. Initially, at intermediate depths, these stress-induced fractured regions are located near the opening perimeter but at great depth the fracturing involves the whole boundary of the excavation.

The analysis of underground openings for stress-induced brittle failure requires knowledge of three variables: the in-situ stress boundary condition, the rock mass strength, and the geometry of the excavation.

The strength of intact rock is determined from laboratory tests on small cylindrical samples and the strength of a rock mass assessed using empirical approaches or by back-analyzing case histories where examples of failure have been carefully documented.

This paper attempts to study the formulae that can be used to assess the stability of pillars in underground openings considering stress-induced brittle failure. We analyze the stability of the pillars with respect to two failure mechanisms: compressive failure, and shear failure of a single plane of weakness.

The study is structured in the following steps:

- Analyze the formulae of classical methods for designing pillars under compression, and standardize said formulae in order to make a comparative study of each method (see Section 2.1).
- Propose a modification of the existing formulae on the basis of the RMR so as to take into account the strength of the rock mass (see Section 2.2).
- Determine pillar safety factors under compression (see Section 3.1) and shearing (see Section 3.2) conditions on the basis of these newly proposed formulae.
- Validate the theoretical results with those obtained in a marble mine located in Alicante (South of Spain), which will allow us to see whether the proposed formulae are applicable to underground marble mines (see Section 4).

2. Methods for Designing Pillars Under Compression

The design of pillars in rock masses can follow three approaches:

- Attempt to numerically simulate the slabbing process using appropriate constitutive models.
- Select a rock mass strength criterion based on the evaluation of rock mass characteristics and calculate the pillar strength to stress ratio at each point using continuum models.
- Use existing empirical pillar stability graphs and pillar formulae.

Despite advances in estimating rock mass strength using rock mass classification systems and advances in our numerical modeling capabilities, pillar design is traditionally carried out using empirical pillar formulae. These formulae were developed from back-analysis of failed pillars in operating mines.

Two primary factors are used in these empirical formulae:

- A shape factor: a geometrical term that represents pillar shape and which is linked to the slenderness of the pillar (the width to height ratio of the pillar).
- A scale factor: a strength term that includes the in-situ rock mass strength.

The empirical formulae employed are basically of two forms:

$$S_p = S_o \cdot \frac{a_p^{\alpha}}{H_p^{\beta}} \tag{1}$$

or

$$S_p = S_o \cdot \left(a + b \cdot \frac{H_p}{a_p}\right), \tag{2}$$

where:

S_p represents the compressive strength of the pillar.
S_o represents the compressive strength of a intact rock sample.
H_p and a_p respectively symbolize the height and width of the pillar.
α, β, a and b are empirical parameters.

We shall first carry out a comparative study of the methods for designing pillars under compression to then propose a modification of such formulae that introduces the effect of the RMR of the rock mass.

2.1 Comparative Analysis of Empirical Methods

The first empirical formulae for designing pillars were developed in coal mining and are therefore applicable to soft rocks: Salamon (1967), Greenwald (1941), and Steart (1954). Their main feature is that the scale effect is minimized by testing a cubic sample of 1 m per side and experimentally determining the value of the compressive strength S_o of said sample.

Table 1. Summarized table of pillar design formulae for hard rocks

Author	Equations	S_o	σ_c	Año	Eq.
Hedley	$S_p = S_o \cdot \frac{a_p^{0.5}}{H_p^{0.75}}$	0.578 σ_c	230 MPa	1972	(3)
Kimmelmann	$S_p = S_o \cdot \frac{a_p^{0.46}}{H_p^{0.66}}$	0.691 σ_c	94 MPa	1984	(4)
Potvin	$S_p = S_o \cdot \frac{a_p}{H_p}$	0.420 σ_c	–	1989	(5)
Krauland	$S_p = S_o \cdot \left(0.778 + 0.222 \cdot \frac{H_p}{a_p}\right)$	0.354 σ_c	100 MPa	1987	(6)
Sjöberg	$S_p = S_o \cdot \left(0.778 + 0.222 \cdot \frac{H_p}{a_p}\right)$	0.308 σ_c	240 MPa	1992	(7)
Lunder-Pakalnis	$S_p = S_o \cdot \left(0.680 + 0.520 \cdot \frac{H_p}{a_p}\right)$	0.440 σ_c	–	1997	(8)
CMRI	$S_p = S_o \cdot \left(\frac{1}{H_p}\right)^{0.36} + \left(\frac{H_p}{250} + 1\right) \cdot \left(\frac{a_p}{H_p} - 1\right)$	0.270 σ_c	–	2000	(9)
Hardy-Agapito	$S_p = S_o \cdot \left(\frac{V_p}{V_s}\right)^{-0.118} \cdot \left(\frac{a_p}{H_p} \cdot \frac{a_s}{H_s}\right)^{0.833}$	σ_c	–	1982	(10)

Other formulae were subsequently developed for hard rocks, in which the scale factor is introduced as a reduction in the uniaxial compressive strength of the intact rock σ_c (varying between 40% and 80%), while the shape factor is considered in a similar way to that described in formulae for soft rocks.

The second column in Table 1 shows the classical formulae of Hedley (1972), Kimmelmann (1984), Potvin (1989), Krauland (1987), Sjöberg (1992) and Lunder-Pakalnis (1997), and the fourth column the average values of the compressive strength σ_c of the materials for which each formula is valid. The third column, S_o, shows the percentage by which σ_c is reduced considering the scale factor.

In order to compare these formulae, they have been standardized on the basis of the uniaxial compressive strength of the rock σ_c for which they were designed. Thus, said strength is considered in Hedley's equation as $\sigma_c = 230$ MPa, in that of Kimmelmann as $\sigma_c = 94$ MPa, in that of Krauland as $\sigma_c = 100$ MPa and in that of Sjöberg as $\sigma_c = 240$ MPa.

Another formula that must also be considered is Eq. (9) of CMRI (Central Mining Research Institute Dhanbad India) used by Sheorey and Singh (2000).

Likewise, Hardy-Agapito (1982) proposed Eq. (10), in which V_p is the volume of the pillar and V_s is the volume of the samples used in the compressive strength test of the intact rock. Said test samples are of width a_s and height H_s.

We compared all these formulae considering a specific case of a 10 m wide square pillar. Figure 1 shows the value of the strength S_p as a function of H_p for all the aforementioned formulae. A uniaxial compressive strength of $\sigma_c = 100$ MPa was considered for the intact rock.

In the above figure, the strength of the pillar exceeds the strength of the intact rock for small pillar heights. For these cases, the shape factor is greater than unity.

The variability of the obtained strengths is worthy of note. If the most conservative formula (CMRI) is compared with the least conservative one (Lunder-Pakalnis), differences in pillar strength of up to 40 MPa are obtained for a pillar height of 10 meters.

Hardy-Agapito and CMRI results are very similar for pillar heights of more than 5 m; it should be borne in mind that heights below this value would be illogical for the

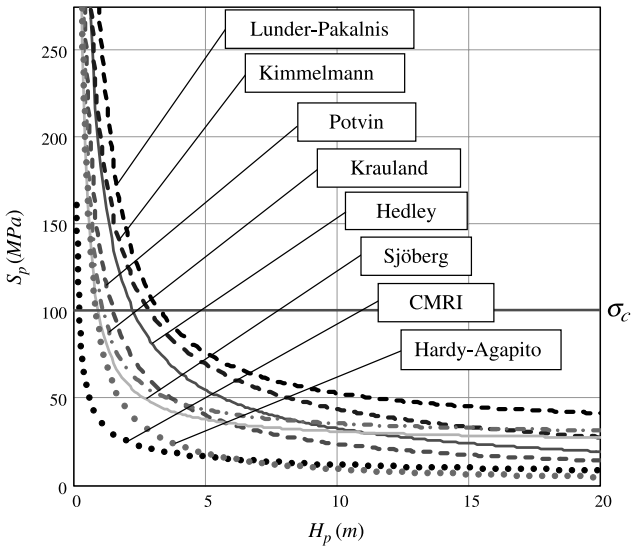

Fig. 1. Variation in the strength of a 10×10 m pillar as a function of its height

width of pillar under consideration, i.e. 10 m. These two formulae are more conservative than the rest and have the added advantage that, although they were designed for hard rocks, they are perfectly applicable to soft rocks and therefore to coal. Hedley's formula, on the other hand, is the one that furnishes average values with respect to those proposed by the set of formulae in Fig. 1.

Henceforth, we shall refer exclusively to these three formulae: Lunder-Pakalnis is the least conservative, CMRI is the most conservative and Hedley gives an average value. Figure 2 illustrates these three formulae.

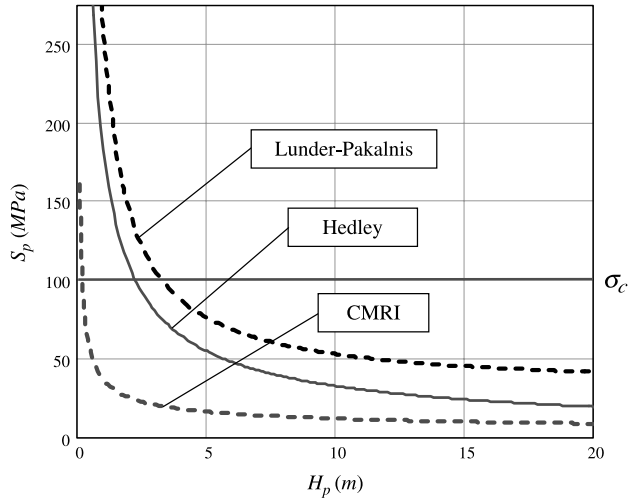

Fig. 2. The most characteristic formulae of pillar strength as a function of height for a 10×10 m pillar

2.2 Modification of the Empirical Methods Taking into Consideration the RMR

In light of the above formulae, the scale effect is taken into account and hence the uniaxial compressive strength of the pillar is reduced due to its difference in size with respect to a laboratory-tested sample. However, the concept of "rock mass" and its quality are not taken into consideration. This gives rise to a serious problem, since the same correction is assigned to a highly fractured rock mass as to a massive one, when the reduction in strength should be much less in the latter case.

To avoid this problem, a new family of formulae is proposed in this paper in which $S_o = \sigma_{cm}$ and the scale effect introduced by the pillar strength is considered as a function of its RMR. To do so, S_o is substituted by the compressive strength of the rock mass σ_{cm} in the three equations that we consider to be the most significant: those of Hedley, CMRI and Lunder-Pakalnis.

Sheorey's failure criterion was chosen to determine σ_{cm} as a function of the RMR (Sheorey, 1997). This criterion establishes that:

$$\sigma_{cm} = \sigma_c \cdot e^{\frac{RMR-100}{20}}. \tag{11}$$

Figure 3 presents the S_p Eq. (3) (considering Hedley) applied to a rock mass made up of hard rock, with σ_c equal to 100 MPa and RMR values of 20, 50, 80, 90 and 100.

The best adjustment between Hedley's classical formula Eq. (11) (using $S_o = 0.578\,\sigma_c$) and the proposed formula (using $S_o = \sigma_{cm}$) is obtained for an RMR close to 90 (although it must be borne in mind that no rock mass made up of rock with a uniaxial compressive strength of 100 MPa can achieve RMR = 90). Hedley's classical formula therefore overestimates the strength of the pillar, above all for medium and low RMR values.

Figure 4 presents the S_p considering Hedley, CMRI and Lunder-Pakalnis with $S_o = \sigma_{cm}$ applied to a rock mass made up of hard rock, with a σ_c equal to 100 MPa and RMR = 50.

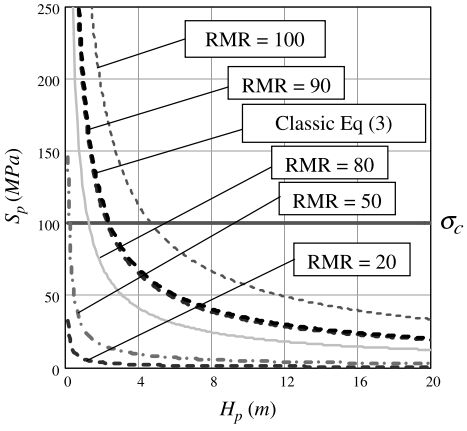

Fig. 3. Strength of the pillar S_p (Eq. (3)) with $S_o = \sigma_{cm}$ for different RMR with $\sigma_c = 100$ MPa

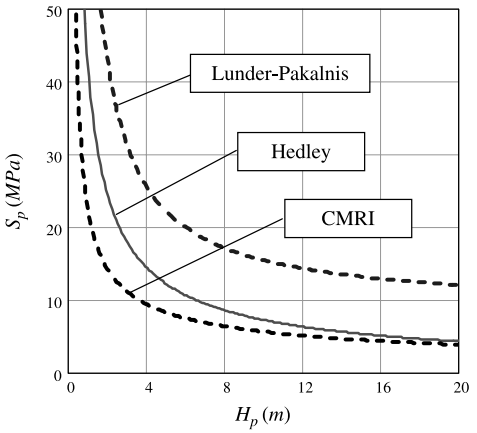

Fig. 4. Strength of the pillar S_p considering $S_o = \sigma_{cm}$ for RMR = 50 with $\sigma_c = 100$ MPa

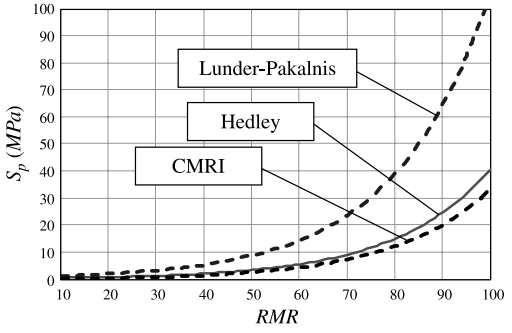

Fig. 5. Comparison of the different formulae for obtaining the strength of a pillar ($\sigma_c = 100$ MPa)

Figure 5 shows the evolution of the strength of a 10 m wide by 20 m high pillar with the RMR of the rock mass considering $\sigma_c = 100$ MPa. It can be seen that when the RMR is 100, Lunder-Pakalnis is the one that best fits the strength of the pillar to that of the intact rock. In this case, Hedley and CMRI are very similar to one another, giving significantly lower values to those of the intact rock.

From the analysis carried out when introducing the RMR in the formulae, it may be deduced that we once more obtain the least conservative pillar design with Lunder-Pakalnis. Hedley takes average values that are very close to CMRI, which is the most conservative.

All the above reasoning leads us to propose Hedley as the most significant formula. However, this would be unwarranted if it were not backed up by a post-analysis of the experimental data in a mine. We therefore studied the safety factors of pillars under conditions of both compression as well as shearing (see Section 3) and validated these safety factors with data measured in a marble mine mined using the room-and-pillar system (see Section 4).

3. Application to Pillar Design

As well as using the above formulae to estimate the side of a pillar to be built, it is also of major interest to know the strength of these pillars once built. Therefore, when evaluating the status of a pillar in a mine, it is best to translate the above formulae into safety factors.

Two types of instabilities were thus taken into consideration in this study:

- Those associated with the collapse of the pillar due to its insufficient compressive strength.
- Those associated with shearing along planes of weakness in the pillar.

Let us now see how the safety factor is defined in each of these two cases.

3.1 The Safety Factor Considering Compressive Failure

Pillar strength S_p is one component that has to be determined when evaluating the stability of a pillar. The other main factor is the load acting on the pillar. The fundamental assumption for the determination of the load on a pillar is that each pillar in a large mined area carries an equal share of the overburden load (Tributary Area Theory), given a regular pillar-panel layout. Strictly speaking, the theory is only valid for those cases in which the span is greater than the mining depth and the mining layout is regular. Regional pillars will affect the load on pillars depending on the span. The average pillar stress σ_{so} according to Tributary Area Theory, is calculated as follows:

$$\sigma_{so} = \frac{(a_p + a_c)^2 \cdot H \cdot \gamma_t}{a_p^2}, \tag{12}$$

where a_p is the width of the pillar and a_c is the stope span, if the ground has a specific weight γ_t and the pillar is located at a depth H.

Of these four factors, the pillar width and span can be controlled, while the mining depth cannot. This formula assumes that the full overburden load is supported by pillars, and the effect of beam bending and stress arching are not considered.

Under these conditions, the safety factor of the pillar under compression is defined as the ratio between its compressive strength S_p and the average pressure σ_{so} that the pillar must support:

$$SF_c = \frac{S_p}{\sigma_{so}}. \tag{13}$$

The numerator of this equation may be obtained using any of the aforementioned formulae, while σ_{so} depends on factors such as overburden, stope span and the width of the pillar itself.

As an example, the dimensions that pillars must have for their compression safety factor to be 3 were calculated. The obtained safety factors are accordingly represented in Fig. 6 as a function of the width of the pillar and its strength. A pillar at a depth of 50 m, a stope span of 20 m, and a pillar height of 20 m were considered. The rock mass has the following properties: $\gamma_t = 27\,\mathrm{KN/m^3}$, $\sigma_c = 100\,\mathrm{MPa}$ and RMR = 75.

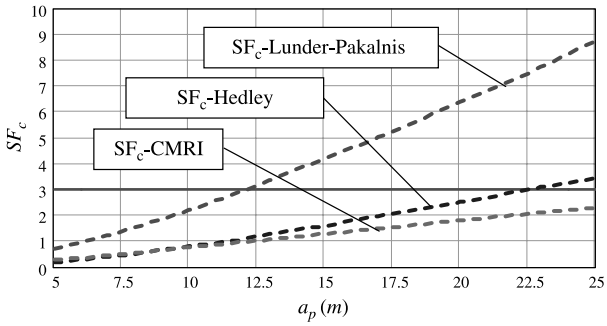

Fig. 6. Compression safety factor of the pillars as a function of their width ($H_p = 20\,\text{m}$)

As can be seen, the smallest pillar (12.5 m) is obtained considering Lunder-Pakalnis, and the largest (over 25 m) using CMRI. Pillars of 22.5 m would be needed using Hedley.

Using a real case, we shall now prove that Hedley gives reliable results for pillar design in underground marble mines (see Section 5). In addition to pillar compressive failure, shear failure is very common in this type of mine. We shall therefore first study how shear failure influences the safety factor so as to be able to correctly interpret pillar failure in the marble mine.

3.2 The Safety Factor Considering Shear Failure

The existence of planes of weakness in the rock mass of the pillar does not only suppose a reduction in σ_{cm} with respect to σ_c; local shear failures may also be produced through one of these planes. This type of failure, which depends on the dip of the joint, is not taken into consideration in the aforementioned methods. However, it should be pointed out that empirical formulae exist (Ramamurthy et al., 1988) that allow σ_{cm} to be determined as a function of the dip of the planes of weakness. These formulae have been tested by researchers such as Esterhuizen (1995) by means of numerical simulations.

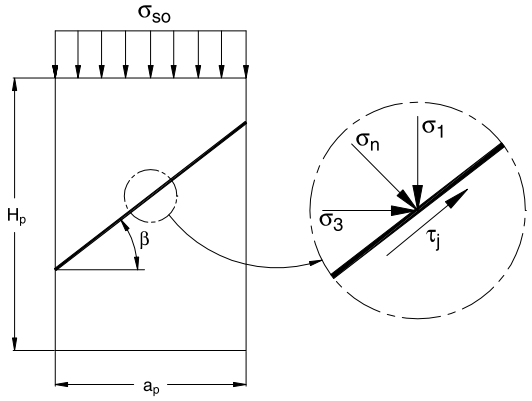

Fig. 7. Pillar affected by a plane of weakness

In this paper, however, the method proposed by Jaeger (1976) was used, since it permits direct introduction of the effect of the orientation of the joints as well as their strength to shear stresses (cohesion and friction).

Figure 7 shows a schematic representation of a pillar of width a_p and height H_p, with a flat plane running through it inclined at an angle of β with respect to the horizontal. Acting on the pillar is an overburden σ_{so}, calculated on the basis of the Tributary Area Theory. The same figure shows a diagram of the stresses acting on the surface of the joint.

The shear safety factor is the ratio between the shear strength of the joint (which is designated as s_j) and the shear stress acting on it (represented as τ_j in the Fig. 7):

$$SF_s = \frac{s_j}{\tau_j}. \tag{14}$$

Likewise, applying Mohr-Coulomb's criterion, s_j is defined as:

$$s_j = c_j + \sigma_n \cdot tg\phi_j, \tag{15}$$

where c_j and ϕ_j are the cohesion and friction angle of the plane of weakness and σ_n represents the set of stresses perpendicular to said plane (see Fig. 8).

Both τ_j and σ_n may be deduced from the principal stresses σ_1 and σ_3 (which, in the case of a vertical pillar, are respectively vertical and horizontal in direction), applying the following relations:

$$\tau_j = \frac{\sigma_1 - \sigma_3}{2} \cdot \sin(2\beta) \tag{16}$$

$$\sigma_n = \frac{\sigma_1 + \sigma_3}{2} + \frac{\sigma_1 - \sigma_3}{2} \cdot \cos(2\beta). \tag{17}$$

Thus, the shear safety factor SF_s results to be:

$$SF_s = \frac{c_j + \left[\frac{\sigma_1+\sigma_3}{2} + \frac{\sigma_1-\sigma_3}{2} \cdot \cos(2\beta)\right] \cdot \tan\phi_j}{\frac{\sigma_1-\sigma_3}{2} \cdot \sin(2\beta)}. \tag{18}$$

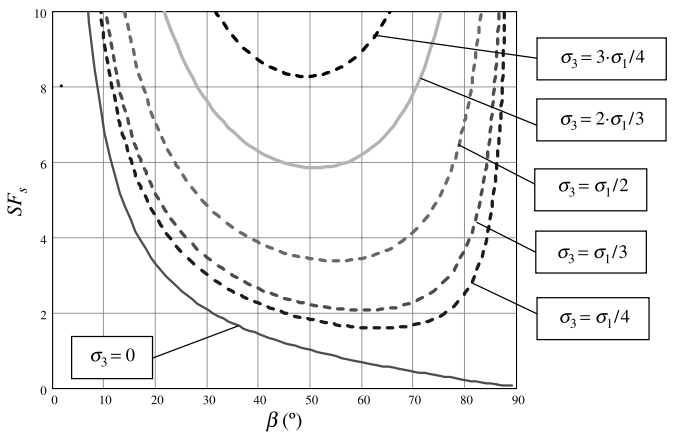

Fig. 8. Safety factor as a function of the dip angle of the joint and of the confinement

Note should be taken in this formula of the influence that the stress state has over the safety factor, and in particular the confinement effect, linked to σ_3. Thus, for any given joint cohesion and friction, and having fixed the vertical stress σ_1, defined on the basis of the overburden of the ground over the pillar, the safety factor will be a function of the angle β and of σ_3.

Figure 8 shows the safety factor versus the dip angle of the joint for different degrees of confinement, defined by the following values of σ_3: 0, $\sigma_1/4$, $\sigma_1/3$, $\sigma_1/2$, $2\sigma_1/3$ and $3\sigma_1/4$. The pillar is assumed to support a stress σ_1 of 10 MPa.

As can be appreciated in Fig. 8, the dip angle of the joint for which the minimum safety factor is obtained varies with the degree of confinement. This slope tends towards 90° when σ_3 tends to zero and decrease as σ_3 increases. To test this fact, the safety factor was minimized as a function of β. The most probable dip angle of the sliding joint in this stress state, $\beta_{\min}$, is thus obtained:

$$\beta_{\min} = \frac{1}{2}\arccos\left[\frac{-(\sigma_1 - \sigma_3)\cdot \tan\phi_j}{1\cdot c_j + (\sigma_1 + \sigma_3)\cdot \tan\phi_j}\right] \tag{19}$$

Figure 9 shows the relation between $\beta_{\min}$ (in degrees) and σ_3 (in kPa) for different cohesion values (10, 500, 1000, 5000, 10000, 50000 and 100000 kPa), considering a friction angle of 45°.

For high values of σ_3 we see that the influence of joint cohesion and friction is practically inexistent, since $\beta_{\min}$ tends to 45°. As σ_3 decreases, the influence of cohesion begins to be appreciated. It can also be observed that the greater the cohesion, the lower the slope of the joint for which the safety factor is found to be minimum; this value tending to 45°.

3.3 Total Safety Factor of the Pillar

The safety factor of the pillar must be determined taking into account two types of possible failure: compression and shearing along the joint. The safety factor of a pillar

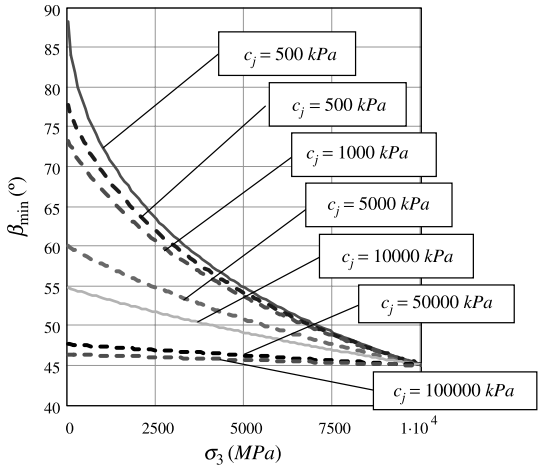

Fig. 9. Dip angle of the joint corresponding to the minimum safety factor $\phi_j = 45°$

will thus be the minimum value between the compression safety factor and the shear safety factor:

$$SF_p = \min[SF_c, SF_s]. \tag{20}$$

Although SF_c is constant for a pillar with a given geometry and depends on the properties of the rock mass, SF_s varies as a function of the characteristics of the planes of weakness.

As an example, we tested the influence of the dip angle of the joint on the safety factor of a pillar in which the geometry and strength properties of the rock mass and the joint remained constant (see Table 2).

On the basis of this data, we first calculate the compression safety factor of the pillar, obtaining the results shown in Table 3.

Table 2. Properties of the pillar

Rock mass properties	$\gamma_t = 27\,\text{kN/m}^3$
	$\sigma_c = 150\,\text{MPa}$
	$\text{RMR} = 75$
Properties of the joint	$c_j = 1\,\text{MPa}$
	$\phi_j = 45^\circ$
Geometrical characteristics	$H_p = 20\,\text{m}$
	$a_p = 15\,\text{m}$
	$a_c = 20\,\text{m}$
	$H = 100\,\text{m}$

Table 3. Results of the strength properties of the rock mass

Stress on the pillar as a function of its tributed area	$\sigma_{so} = 7.35\,\text{MPa}$
Compressive strength of the rock mass using Sheorey	$\sigma_{cm} = 28.65\,\text{MPa}$
Compressive strength of the pillar (using Hedley)	$S_p = 11.73\,\text{MPa}$
Compression safety factor of the pillar	$SF_c = 1.2$

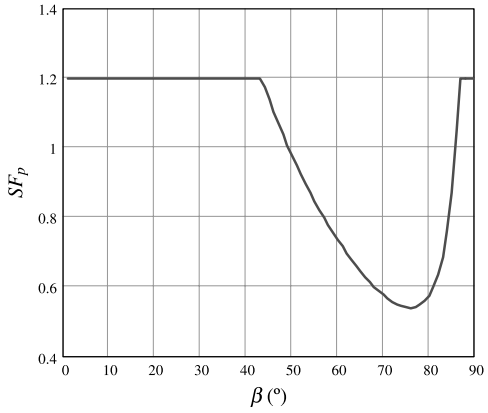

Fig. 10. Safety factor of the pillar as a function of β

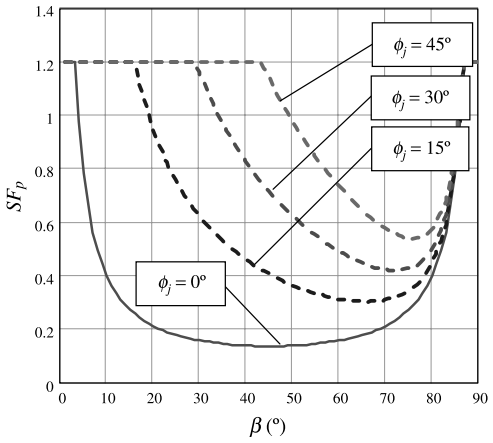

Fig. 11. Safety factor of the pillar as a function of β for different ϕ_j

Figure 10 shows the safety factor of a pillar as a function of the dip angle β of its joints, considering the strength properties in Tables 2 and 3.

It can be seen that for dip angles less than 44°, failure of the pillar is conditioned by its compressive strength, whereas for slopes of between 44 and 87°, failure would be produced due to shearing. The slope of the joint for which the safety factor is minimum is, in this case, 76°.

The shear safety factor of the pillar and the slope β that gives the minimum safety factor vary with the friction angle of the joint, as can be seen in Fig. 11, which shows the curves corresponding to friction angles of 0°, 15°, 30° and 45°.

We can see that $\beta_{\min}$ increases with ϕ_j. For a friction angle of 0°, $\beta_{\min}$ is 45° and for a friction angle of 45°, the value of $\beta_{\min}$ is 78°.

4. Validation in the Design of Marble Pillars

In this section we shall validate the design formulae proposed when introducing the RMR effect and shall see which of these formulae best fits a marble mine. The mine in which the study was carried out is a marble mine located in Alicante (Southern Spain) mined by room-and-pillar method. This mine was chosen because it presents very uniform pillars in which the RMR is easy to calculate.

Mining is carried out on two levels, an upper level named PSUP and a lower level named PINF, with a length of 325 m and a width of 200 m per level. The upper level is located at an average depth of 100 meters and the lower level at a depth of 150 meters. Figures 12 and 13 show the shape and layout of each one of the pillars in level PSUP and level PINF.

The dimensions of the rooms and pillars are highly variable. They have an average height of 17 m in PSUP and of 14 m in PINF, although in many case they exceed 20 m, even reaching 24 m. The average room span is 18 m, while the width of the pillar usually varies between 8 and 22 m.

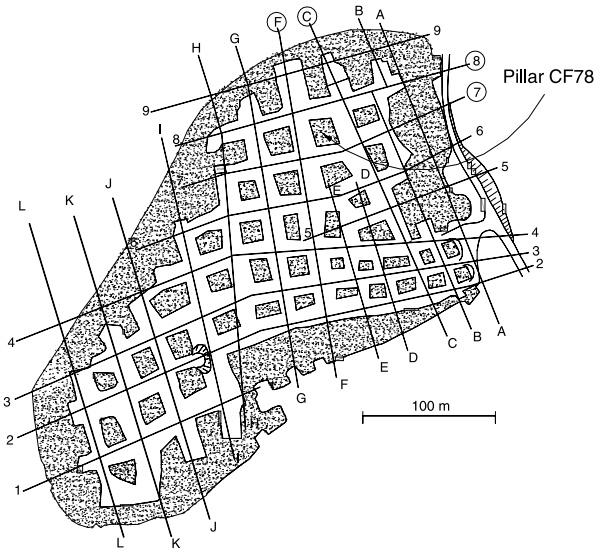

Fig. 12. Location plan of the pillars in the upper level PSUP

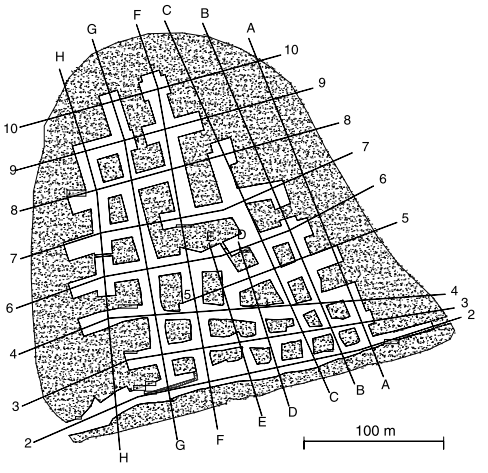

Fig. 13. Location plan of the pillars in the lower level PINF

In order to identify it, each pillar was given a name made up of two letters (A, B, C, D, etc.) and two numbers (1, 2, 3, etc.), taking as a reference the longitudinal and transversal alignments drawn in Figs. 12 and 13. For example, pillar CF78 is situated between the longitudinal alignments C and F and the transversal alignments 7 and 8 (see Fig. 12).

We shall first see the typology of the existing pillars, describing their appearance and the way in which failure is produced in these pillars, when it exists. We shall subsequently see how the rock mass of the mine is characterized and then proceed to

analyze the safety factors obtained for each pillar. Finally, we shall set out the points of agreement and the discrepancies observed between the apparent status of each pillar and the numerical values obtained.

4.1 Apparent Status of the Pillars

After exhaustive inspection of all the pillars of the mine, four statuses may be distinguished among the pillars: stable, exhibiting corner failure, exhibiting lateral failures and manifest failure:

- *Corner failure*: The vast majority of pillars present damage to their corners with the subsequent tendency towards roundness (see Fig. 14). This is slight damage and, within the scope of this study, these pillars were considered as stable.
- *Lateral failures*: Lateral (chip-type) fractures are more important, giving rise to pillars with some of their faces chipped. This type of damage, shown in Fig. 15, corresponds to incipient-type failure, and is produced when the failure of the two consecutive corners progresses until converging, thus affecting an entire face of the pillar.
- *Manifest failure*: This is produced when the fractures, of a much greater magnitude, traverse the pillar completely, either sub-vertically or at an angle of 45°. This type of failure develops when lateral failure progresses until practically affecting the

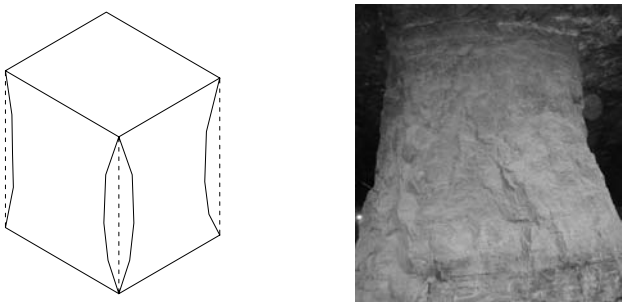

Fig. 14. Pillar with corner damage (pillar BC27 level PSUP)

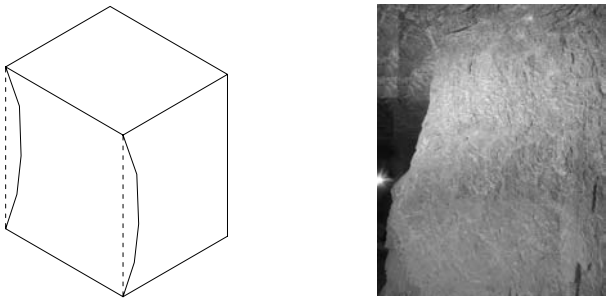

Fig. 15. Pillar with lateral damage (pillar FG67 level PSUP)

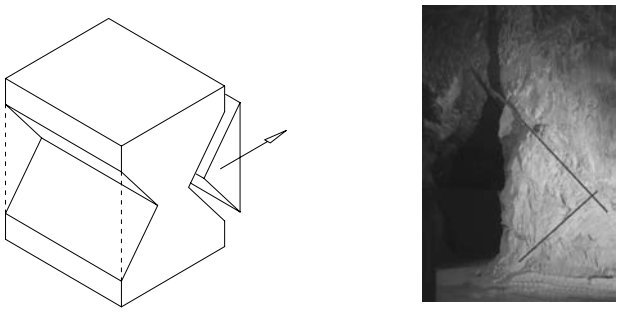

Fig. 16. Failed pillar with a 45° fracture (pillar GH67 level PINF)

pillar nucleus, which then enters into manifest failure. Figure 16 shows an example of this type of damage.

It should be borne in mind that failure of a pillar leads to overburden on the adjacent pillars, especially in those that already present incipient failures. The overburden is transmitted in this way from pillar to pillar, possibly producing a failure chain reaction or domino effect.

4.2 Rock Mass and Pillar Characteristics

Table 4 presents a summary of the parameters considered in the calculation of the RMR in the rock mass of the level PSUP. The RMR varied between 61 and 74.

Table 5 presents a summary of the parameters considered in the calculation of the RMR in the rock mass of the level PINF. In this case, the RMR varied between 50 and 79.

Besides the value of the uniaxial compressive strength, one of the factors that most conditions the final value of the RMR is the condition of the joints, since for similar values of RQD, these are what establish the differences between the different classes of rock masses. Comparing the characteristics assigned to the joints on level PSUP with those of level PINF, it can be seen how much more unfavorable situations of rock mass stability may arise: much larger apertures, the absence of roughness and soft

Table 4. Parameters for calculating the RMR (level PSUP)

Parameter	Condition	Evaluation	RMR
Uniaxial compressive strength (σ_c)	61 MPa	7	61 ÷ 74
RQD	75 ÷ 90%	17	
Joint spacing	20 ÷ 60 cm	10	
Condition of the joints			
Persistence	3 ÷ 10 m	2	
Aperture	None ÷ 1–5 mm	6 ÷ 1	
Roughness	Rough	5	
Filling	Hard <5 mm ÷ None	4 ÷ 6	
Weathering	Somewhat weathered ÷ None	5 ÷ 6	
Water	Damp patches ÷ Dry	10 ÷ 15	

Table 5. Parameters for calculating the RMR (level PINF)

Parameter	Condition	Evaluation	RMR
Uniaxial compressive strength (σ_c)	104 MPa	12	50 ÷ 79
RQD	75 ÷ 90%	17	
Joint spacing	20 ÷ 60 cm	10	
Condition of the joints			
Persistence	3 ÷ 10 m	2	
Aperture	None ÷ 5 cm	6 ÷ 0	
Roughness	Smooth ÷ Rough	0 ÷ 5	
Filling	Soft >5 mm ÷ None	0 ÷ 6	
Weathering	Somewhat weathered ÷ None	5 ÷ 6	
Water	Dripping ÷ Dry	4 ÷ 15	

fillings that favor sliding processes. When all these situations coincide, the value of the RMR decreases considerably. Table 6 shows the RMR assigned to each pillar along with the most characteristic geometrical parameters (H pillar depth, H_p pillar height and a_p pillar width).

Table 6. Geometrical parameters and the RMR of each pillar

Pillar	$H(m)$	$H_p(m)$	$a_p(m)$	RMR
Level PSUP				
AB23	3.0	11.00	10.00	67
AB34	2.0	11.00	9.00	71
BC23	22.0	10.00	12.00	74
BC34	17.5	11.00	8.00	66
BC67	36.0	23.50	11.00	64
BC78	47.0	19.00	17.00	61
CD23	41.0	13.25	14.00	63
CD34	36.0	13.50	19.00	64
CE45	43.0	14.25	23.00	77
CE56	48.0	20.25	12.00	75
CF67	67.0	19.00	19.00	67
CF78	69.0	19.00	17.00	68
DE23	60.0	14.00	12.00	67
DE34	62.0	15.00	10.00	67
EF23	81.0	14.50	16.00	68
EF34	74.0	17.75	9.00	72
EF46	65.0	17.75	11.00	73
FG23	104.0	12.50	14.00	74
FG34	97.0	15.75	14.00	66
FG46	98.0	17.00	10.00	64
FG67	93.0	15.00	17.00	64
FG78	94.0	14.00	19.00	72
GH23	127.0	12.25	18.00	66
GH34	120.0	15.00	13.00	66
GH46	123.0	16.25	16.00	74
GH67	121.0	16.50	13.00	66
HI23	151.0	14.00	17.00	66
HI34	151.0	14.00	16.00	64
HI46	158.0	12.75	19.00	72
IJ12	181.0	24.00	19.00	74

(*continued*)

Table 6 (*continued*)

Pillar	$H(m)$	$H_p(m)$	$a_p(m)$	RMR
IJ23	181.0	24.00	16.00	72
IJ34	194.5	13.50	27.00	73
JK12	176.0	16.00	17.00	67
JK23	195.6	16.00	15.00	74
KL01	159.0	16.00	19.00	61
KL12	167.5	16.00	14.00	71
KL23	187.5	16.00	15.00	61
Level PINF				
AB23	85.0	16.50	12.00	69
AB34	83.0	17.25	13.00	73
BC23	104.0	18.50	15.00	60
BC34	105.0	17.25	8.50	54
BC45	103.0	17.50	11.00	60
BC56	106.0	16.25	11.00	60
BC67	108.0	12.75	17.00	64
CD23	120.0	17.50	14.00	64
CD34	122.0	17.25	19.00	67
CE45	130.0	18.75	26.00	68
CE56	133.5	12.50	15.50	50
DE23	150.0	13.00	61.00	55
DF34	151.0	17.25	12.00	55
EF23	170.0	15.00	32.00	53
EF46	170.5	14.50	23.00	60
FG23	191.0	14.00	14.00	60
FG34	198.0	12.00	15.00	60
FG46	193.5	16.00	18.00	50
FG78	193.0	19.25	15.50	70
FG89	192.0	8.00	21.50	55
GH46	210.0	7.00	21.00	55
GH67	214.0	14.25	18.00	60
GH78	219.0	13.00	17.00	79
GH89	217.0	7.75	11.00	60

In those pillars affected by planes of weakness, the values of cohesion and friction angle obtained by direct shear testing were taken into account. It should be noted that these values are only valid until shearing starts to occur. Once the movement has begun, both values decrease considerably, friction possibly being reduced to less than a half.

4.3 Pillar Safety Factors

The safety factors were determined in accordance with the following method:

- The 37 pillars on level PSUP of the mine and the 24 pillars on level PINF were analyzed so as to define their actual status.
- The strength of each pillar was obtained using the formula in Eq. (3) with $S_o = \sigma_{cm}$, considering Sheorey's failure criterion Eq. (11) of the rock mass.
- The compression safety factors were determined using Eq. (13) and the shear safety factors using Eq. (18).

- The range of values of the safety factor Eq. (20) was determined for stable pillars, pillars with initial status of failure and pillars showing manifest failure.
- Those pillars that did not fit said range of safety factor were analyzed with the aim of justifying their status.

Table 7 shows the values obtained for each pillar of the compression and shear safety factors, together with an evaluation of the actual status of the pillar. When no numerical

Table 7. Safety factors and real status of the pillars

Pillar	SF_c	SF_s	Pillar status
Level PSUP			
AB23	43.93	–	Stable
AB34	50.47	–	Stable
BC23	7.94	–	Stable
BC34	7.76	–	Stable
BC67	2.36	–	Stable
BC78	2.81	–	Stable
CD23	3.62	–	Stable
CD34	3.91	–	Stable
DE23	2.54	–	Stable
DE34	1.39	–	Failed
EF23	0.87	–	Incipient failure
EF34	0.79	–	Failed
CE45	4.08	–	Stable
CE56	1.79	–	Stable
EF46	1.65	–	Stable
CF67	1.90	–	Stable
CF78	2.44	–	Stable
FG23	1.08	–	Incipient failure
FG34	1.50	–	Stable
FG46	1.08	–	Incipient failure
FG67	2.07	–	Stable
FG78	2.47	–	Stable
GH23	0.91	–	Incipient failure
GH34	1.25	–	Stable
GH46	1.30	–	Incipient failure
GH67	0.96	–	Incipient failure
HI23	1.05	–	Stable
HI34	0.96	–	Incipient failure
HI46	1.39	–	Stable
IJ12	0.98	–	Incipient failure
IJ23	1.00	–	Incipient failure
IJ34	1.30	–	Stable
JK12	1.55	–	Stable
JK23	1.68	–	Stable
KL01	1.73	–	Stable
KL12	1.36	–	Stable
KL23	0.82	–	Incipient failure
Level PINF			
AB23	6.14	–	Stable
AB34	6.06	–	Stable
BC23	4.02	–	Stable
BC34	2.89	–	Stable

(*continued*)

Table 7 (*continued*)

Pillar	SF_c	SF_s	Pillar status
BC45	3.06	–	Stable
BC56	2.20	–	Stable
BC67	5.37	–	Stable
CD23	2.91	–	Stable
CD34	2.63	–	Stable
CE45	3.51	–	Stable
CE56	2.73	–	Stable
DE23	1.85	–	Stable
EF23	1.06	–	Incipient failure
DF34	7.29	1.88	Incipient failure
EF46	1.74	–	Stable
FG23	0.83	–	Incipient failure
FG34	1.29	–	Incipient failure
FG46	1.36	–	Stable
FG78	2.50	–	Stable
FG89	1.99	–	Stable
GH46	1.15	0.71	Failed
GH67	1.14	0.70	Incipient failure
GH78	0.94	–	Failed
GH89	1.42	1.04	Incipient failure

value of the shear safety factor is given, this is because no shear plane of weakness was observed. Those pillars in which the real status does not correspond to the safety factor are shaded in Table 7. We shall study each pillar in the next section of the paper.

4.4 Evaluation of the Status of the Pillars

As regards marble mines with similar characteristics to those indicated here, we may conclude that:

- Those pillars that have a safety factor greater than 1.25 do not present problems of stability, provided that the adjacent pillars are not damaged.
- Pillars with a safety factor between 0.90 and 1.25 present a state of incipient failure.
- Pillars with a safety factor below 0.90 present a state of manifest failure (unless they are located at the edge of the stope).

Taking these criteria into account, we obtain the pillar failure status classification shown in Figs. 17 and 18. Those pillars not identified with any symbol are stable.

Specific pillars exist for which a certain disparity may be appreciated between their actual status and the theoretical classification of the pillars as a function of their safety factor. These pillars are shaded in Table 7 and correspond to two types of anomalous situations:

- Pillars with apparently high compression safety factors, but which are in fact damaged.
- Pillars with a compression safety factor lower than 1 that are not actually as damaged as they theoretically should be, given their low safety factor.

To understand these anomalies, an individualized pillar-by-pillar study is required that takes into account their evolution over time. Thus, for the pillars on level PSUP,

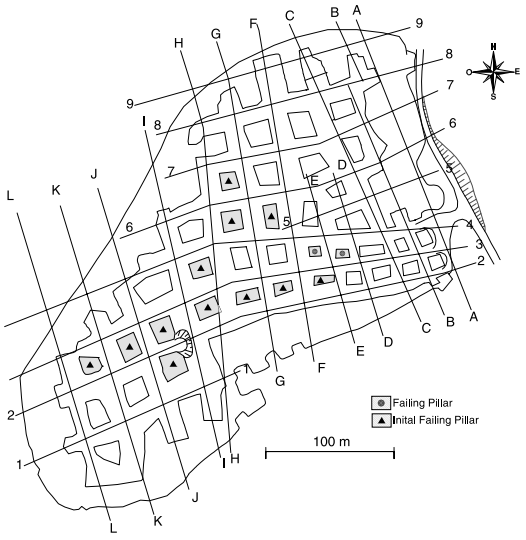

Fig. 17. Location of the failed pillars on level PSUP

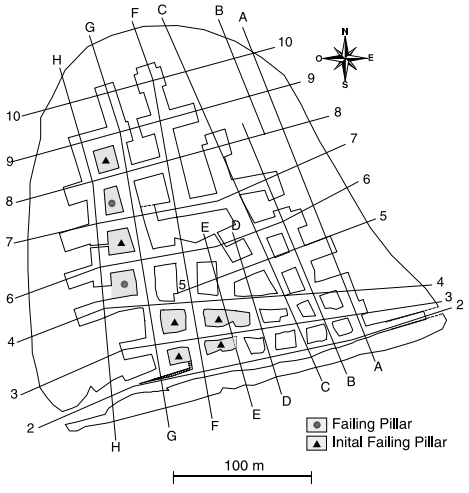

Fig. 18. Location of the failed pillars on level PINF

we find that:

- The failure of pillar DE34 responds to the excess load to which it was subjected as a consequence of the failure of the adjacent pillar (EF34), whose reduced dimensions are insufficient to support the weight of the overhanging cover. The same explanation is applicable to pillar GH46, the failure of which is due to its being situated next to two damaged pillars (FG46 and GH67).
- Pillars EF23 and KL23 present compression safety factors of 0.87 and 0.82 respectively, which indicates that they should present failure. However, they are still in a

state of incipient failure. This fact is justified by their being situated at the edge of the stope, which acts like a large-sized pillar, thus freeing them of part of their load. The same effect is produced for pillar HI23.

The following anomalies were observed for the pillars on level PINF.

- Pillar GH46 is traversed by 45° joints, which necessitates the calculation of its shear safety factor. Thus, although the compression safety factor is high, its shear safety factor is very low, thereby provoking its failure via a plane of weakness.
- In the case of pillar GH67, although the initial conditions are very similar to those of pillar GH46, shear failure is not produced due to its being located between the edge of the stope and a large-sized pillar, which helps it support part of its load.
- Pillar GH89 has sufficient compressive strength and its shear safety factor is at the limit of stability. However, the pillar is in a process of incipient failure. This is due to the presence in this pillar of a fault with serpentine filling with a very low internal friction angle (see Fig. 19). The position of this pillar next to the edge of the stope helps impede its total collapse.
- Pillar GH78 does not present any fractures that might provoke shearing and the compression safety factor indicates a state of incipient failure; however, the pillar is very damaged. This is probably due to the excess load that the pillar has to support as a consequence of the damage to the adjacent pillars GH89 and GH67. The fact that it is not in a worse state than the one it presents is undoubtedly due to its being situated between an area at the edge of the stope and a large extended pillar, which helps to support part of its load.
- Despite having a compression safety factor of 0.89, pillar FG23 is still in a state of incipient failure. This is justified by its situation next to a stope edge, which frees it of part of its load.
- As regards pillar FG34, it may be stated that the state of incipient failure in which it is to be found is a result of the damage suffered by the adjacent pillars.
- Although pillar DF34 has very high compressive and shear safety factors, it is in a process of incipient shear failure owing to the damage suffered by the adjacent pillars.

Fig. 19. Detail of the sliding plane of the serpentine filling in pillar GH89

5. Conclusions

The introduction of the RMR effect in classical pillar design formulae allows a more accurate study of compressive failure in pillars. On the basis of the comparative analysis carried out, the conclusion may be drawn that classical methods overestimate pillar strength for medium and low RMR. This error has traditionally been offset by the application of high safety factors.

On the other hand, the proposed method based on Hedley (with $S_o = \sigma_{cm}$) allows the safety factor of pillars in a mine to be determined with great reliability, provided that the pillars are isolated. The method is not appropriate for pillars at stope edges or when a pillar is affected by the collapse of one or other of its adjacent pillars.

In the case of marble mines similar to the one studied in this paper, the following classification of pillars may be established on the basis of their safety factor: $SF > 1.25$: stable pillars, $0.90 < SF < 1.25$: stable pillars with incipient damage and $SF < 0.90$: pillars with manifest failure.

Acknowledgements

The authors gratefully acknowledge the assistance of Paul Barnes in the preparation of this paper in English.

References

Esterhuizen, G. S. (1995): Investigation into the effect of discontinuities on the strength of coal pillars. Technical Papers. Safety in Mines Research Advisory Committee Symposium. The South African Institute of Mining and Metallurgy.

Greenwald, H. P., Howarth, H. C., Hartmann, I. (1941): Progress Report: Experiments on strength of small pillars of coal in the Pittsburgh bed. USBM, R. I. 3575.

Hardy, P., Agapito, J. F. T. (1982): Induced horizontal stress method of pillar design in oil shale. XV Oil Shale Symp. Colorado School of Mines, Golden, Colorado.

Hedley, D. G. F., Grant, F. (1972): Stope-and-pillar design for the Elliot Lake Uranium Mines. Bull. Can. Inst. Min. Metallurg. 63, 37–44.

Jaeger, J. C., Cook, N. G. W. (1976): Fundamentals of rock mechanics. Chapman Hall, London.

Kimmelmann, M. R., Hyde, B., Madgwick, R. J. (1984): The use of computer applications at BCL limited in planning pillar extraction and design of mining layouts. In: Proc., ISMR Symp. Design and Performance of Underground Excavations. Brit. Geotech. Soc., London, 53–63.

Krauland, N., Soder, P. E. (1987): Determinating pillar strength from pillar failure observations. Eng. Min. J. 8, 34–40.

Lunder, P. J., Pakalnis, R. (1997): Determination of the strength of hard-rock mine pillars. Bull. Can. Inst. Min. Metall. 90, 51–59.

Potvin, Y., Hudyma, M. R., Miller, H. D. S. (1989): Design guidelines for open stope support. Bull. Can. Min. Metall. 82, 53–62.

Ramamurthy, T., Rao, G. V., Singh, J. A. (1988): A strength criterion for anisotropic rock. In: Proc., 5th Australia-New Zealand Conf. on Geomechanics. Sydney, vol. 1, 253–257.

Salamon, M. D. G., Munro, A. H. (1967): A study of the strength of coal pillars. J. S. Afr. Inst. Min. Metall. 67, 56–67.

Sheorey, P. R., Loui, J. P., Singh, K. B., Singh, S. K. (2000): Ground subsidence observations and a modified influence function method for complete subsidence prediction. Int. J. Rock Mech. Min. Sci. 37, 801–818.

Sheorey, P. R. (1997): Empirical rock failure criteria. A. A. Balkema Publ., Rotterdam.

Sjöberg, J. (1992): Failure modes and pillar behaviour in the Zinkgruvan mine. In: Proc., 33° U.S. Rock Mech. Symp., Santa Fe. A. A. Balkema Publ., Rotterdam, 491–500.

Steart, F. A. (1954): Strength and stability of pillars in coal mines. J. Chem. Metall. Min. Soc. SA, 54: 309–325.

Authors' address: Dr. C. González-Nicieza, Department of Mining Engineering, Mining Engineering School, University of Oviedo, Independencia 13, 33004 Oviedo, Asturias, Spain; e-mail: celes@git.uniovi.es